

# Investigation of the Effects of Fuel Cells on V-Q & V-P Characteristics

Mahmoud Zadehbagheri<sup>1</sup>, Mohammad Javad Kiani<sup>2</sup>, Tole Sutikno<sup>3,4</sup>

<sup>1,2</sup> Department of Electrical Engineering, Islamic Azad University, Yasouj Branch, Yasouj, Iran

<sup>3</sup> Department of Electrical Engineering, Universitas Ahmad Dahlan, Yogyakarta, Indonesia

<sup>4</sup> Embedded System and Power Electronics Research Group, Yogyakarta, Indonesia

Email: <sup>1</sup> ma.zadehbagheri@iau.ac.ir, <sup>2</sup> kianiph@gmail.com, <sup>3</sup> tole@ee.uad.ac.id

\* Corresponding author

**Abstract**— In this paper, the use of a FC system connected to the network is proposed as a source of DG with high reliability, and for this purpose, the dynamic model of the fuel cell has been simulated. A hybrid system of fuel cell distributed generation (FCDG) is presented to provide electrical energy for a small isolated area. Boost converter (DC/DC), in order to increase the voltage level of the system and stabilize the DC link voltage has been used, which provides the possibility of connecting several different scattered production sources in parallel. Voltage stability is concerned with the ability of a power system to maintain acceptable bus voltages under normal conditions and after being subjected to a disturbance. The use of DG sources has many advantages, including meeting peak load needs, reducing network losses, providing reactive power locally, and regulating network voltage. Among all sources of distributed production, fuel cells are of special importance due to their high efficiency, high energy density, the ability to simultaneously produce heat and electric power, and low emission of pollutants. Using fuel cells (FCs) have several advantages and in this paper we investigate the effects of FCs on power systems via simulation a single machine (DG as small gas turbine coupled with a FC) in the Dig Silent area for different PF of FC. Different PF for FC obtained with control the DC to AC inverter. We found that by control the PF of FCs, we can increase the limitation of reactive generation of overall system and improve the V-P & V-Q characteristics of overall system. With the grid-connected inverter's switching control, the active and reactive power injected into the grid is controlled independently.

**Keywords**— Fuel Cell (FC), Voltage Stability, Distributed Generation (DG), Dig Silent, Voltage Collapse, Power Active, Power Reactive, Vector Control., Proton Exchange Membrane (PEM).

## I. INTRODUCTION

In recent years, significant progress has been made in the field of using DG resources connected to the distribution network. Advantages such as reducing the losses of power distribution lines, correcting the voltage profile locally (strengthening the network) and reliable supply of peak load by small production units instead of large power plants have led to extensive studies in the field of their types and control [1]. Among all the available options for use as a distributed generation source, there are significant advantages such as the possibility of simultaneous production of electricity and heat, high efficiency (due to the direct conversion of chemical energy into electricity), negligible emission of environmental pollutants and very high energy density.

(About 10 times of common batteries), has caused fuel cells to be considered as the most important source of distributed production in the future of the world's energy industry. High energy density means the possibility of long-term supply of load considering the low energy density of the batteries, this work is not practical with the battery set. On the other hand, as long as a FC is fed by the input hydrogen, it will be possible to continuously produce electric power like a diesel generator, with the difference that unlike an internal combustion engine, energy conversion takes place with high efficiency and negligible emission of pollutants. Therefore, it can be said that a FC has the positive characteristics of a battery and a diesel generator at the same time. The main difference between the types of FCs is the type of electrolyte used in their construction.

In reference [2], studies on the combined system of fuel cell and battery in vehicle applications are presented. In this system, the controller is used to manage the power distribution. The main purpose of the controller in this article is to stabilize the DC bus voltage and set the battery charging mode within the permissible range. In reference [3], studies have been done in connection with the combined system of fuel cell and supercapacitor in vehicle applications. The main focus in this study is on the fuzzy controller algorithm, which is able to determine the amount of power required from the fuel cell and maintain the DC bus voltage within the nominal range. In reference [4], they presented the combination of fuel cell with battery and supercapacitor in hybrid electric cars. In such a combination, by providing a smart strategy and a fuzzy controller, optimal energy management in the power sources of the hybrid fuel cell vehicle has been investigated. The results of this study showed that maintaining the state of battery and supercapacitor charge improves dynamic performance and increases efficiency in terms of fuel savings.

In reference [5], they presented the use of a photovoltaic (PV) system to produce hydrogen and a FC system to provide heat and electricity. In this article, the technical and economic feasibility of using a combined photovoltaic-fuel cell (PVFC) system in residential applications for the simultaneous production of electricity and heat has been investigated. The technical and economic analysis was investigated and it was shown that currently, the PV system



is the most economical combined system, but the use of a FC next to this system in residential applications is not justified. It is predicted that with the increase in the price of energy carriers as well as the decrease in the cost of installation and commissioning, fuel cell systems will be economical in the future.

In reference [6], they presented an article for bidirectional converter control in a hybrid system based on a polymer FC. In which, the desired controller to control the bidirectional converter is the sliding mode control, which is a non-linear controller and resistant to any type of disturbance, but the system used in this article consists only of the FC system and the combined system of the FC and The battery is not used. In reference [7, 8], The polymer FC energy is used as the main power source, while the lead acid battery is considered as the auxiliary power source. Due to the slow dynamics of the FC system, the auxiliary power source of the lead-acid battery has been used for use in DGs. In order to use this hybrid system, an algorithm was presented that describes how to supply the load and charge and discharge the battery [9, 10]. In this algorithm, if the power required by the load is less than the power produced by the FC, then the entire load is supplied by the FC. But if the required power of the load is more than the production power of the FC, then this lack of power must be provided according to the state of charge of the battery and the rated power of the battery. But if the power required by the load is less than the power produced by the FC, this additional power is used to charge the battery.

In reference [11], a real system in Japan was used to implement the proposed control method with the aim of improving the technical dimensions of the network. Therefore, in this reference, by adding a FC scattered production source, providing heat loads is also It has been considered and in addition to considering controllers and previous optimization goals, fuel costs have also been considered. In this comprehensive control method, in addition to the control variables related to the devices used in the network, the production power of resources is also used as a control variable to reduce costs and pollution [9, 12].

## II. FC OVERVIEW

Features such as the high efficiency of FCs, the proper performance of these sources at variable load, low pollution, noiselessness, no moving parts, the variety of fuels used and the wide range of capacity of these sources can be mentioned as the main reasons for the desire to use them. On the other hand, the high construction costs of these resources have made their use in many applications uneconomical [13]. From another aspect, there are no necessary economic incentives for the use of these resources by private investors, and due to the high construction costs, the investor will not have a suitable return rate. Researchers, builders and energy companies in different parts of the world are trying to develop these resources technically and economically and make them available with lower construction costs and higher efficiency [14]. Methods such as guaranteed purchases with specific prices, along with these efforts, are common support measures in many regions

of the world. With the beginning of the 21st century, fuel cells have become prominent in various applications in power supply [15, 16]. A fuel cell is an electrochemical device that directly converts chemical energy into electrical energy. Technically speaking, fuel cells can be used in a wide range of applications from providing energy for a portable electronic component to a large energy unit in an electric company [17].

Among the technologies that can play an important role in this period of transition are fuel cells. Although this technology has a history of more than one hundred and fifty years, it has not been able to compete with traditional methods of energy conversion due to various issues, including the high cost. Of course, rapid developments in this technology draw a very bright horizon for it. With the use of fuel cells, the issue of hydrogen production and its storage methods as a fuel used in fuel cells becomes of special importance in such a way that many analysts call the energy sector of the future economy based on hydrogen instead of carbon [18, 19]. Some types of fuel cells, such as SOFC and MCFC, have a time to reach high operating temperature and as a result, a lower response speed, so they are suitable for powering building units and large transportation vehicles such as ships and locomotives. On the other hand, the PEMFC type fuel cell has a low operating temperature and a high response speed, and is suitable for providing the energy needed by cars that have instantaneous operation [20].

Furthermore, using high-temperature fuel cells also, cogeneration heat makes those appropriate for residential, commercial, or industrial applications, where electricity and heat generation are needed simultaneously Since entering the new century, Fuel cell technologies have grown exponentially in recent years, as shown Fig. 1. Fuel cells can be coupled with a micro gas turbine, small gas turbine and HRSG for production electricity and heat have a higher efficiency if both are used [21].

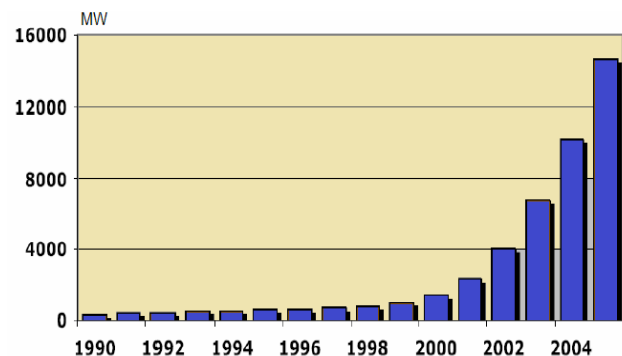


Fig. 1. Cumulative installed FC units worldwide, 1990-2005

### 1.2. Modeling of FC

A fuel cell converts chemical energy directly into electrical energy. There are three types of losses in a fuel cell: activation losses - Ohmic losses - concentration losses. The polarization curve of the FC showing its losses is shown in Fig. 2 [22].

The parameters of the polymer FC system model are shown in Table 1. The ideal voltage of a hydrogen/oxygen

FC, under the standard conditions of one atmosphere and 25 degrees Celsius, is equal to 1.229 volts. But the actual voltage of the FC is lower than its ideal voltage. Because the voltage drop occurs in the FC. Considering this voltage drop, the output voltage of the fuel cell is expressed by the following expression [23, 24].

$$V_{FC} = E_{ernst} - V_{act} - V_{conc} - V_{ohmic} \quad (1)$$

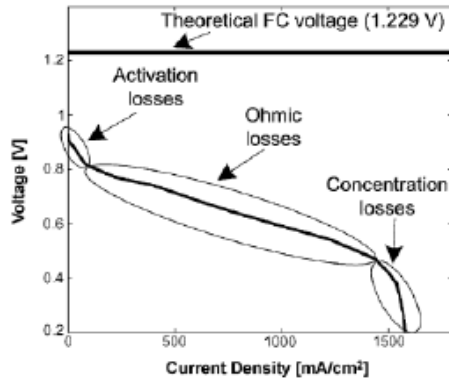


Fig. 2. FC polarization curve (V-I curve) [5]

According to equation 1, the instantaneous Nernst voltage ( $E_{ernst}$ ) is written as follows: [25]

$$E_{ernst} = 1.229 - (8.5 \times 10^{-4})(T - 298.15) + 4.308 \times 10^{-5} T \times \ln(P_{H_2} + 1/2 P_{O_2}) \quad (2)$$

Activation loss is related to the amount of energy that the catalyst consumes to start the reaction [26]. The effect of activation losses on the cell voltage can be shown as follows [13].

$$V_{act} = \eta + a.(T - 298) + T.b.\ln(I) \quad (3)$$

Where,  $\eta$ ,  $a$  and  $b$  the constant values are in volts, volts per kelvin and volts per kelvin ampere respectively [27].

TABLE I. MODEL PARAMETERS OF POLYMER FC SYSTEM

A	Activation Area (cm <sup>2</sup> )	R <sub>a</sub>	Equivalent Resistance
B	Constant	K <sub>o2</sub>	Molar Constant, O <sub>2</sub>
C	Capacitance	K <sub>H2</sub>	Molar Constant, H <sub>2</sub>
Co <sub>2</sub>	Oxygen Concentration	R <sub>ohmic</sub>	Internal Resistance
E <sub>ernst</sub>	Instantaneous Voltage	T (k°)	FC Temperature
F	Farad Constant	To, Tic, Tit, Trt	Experimental Parameters
IFC	FC Current (A)	U	Consumption Factor
J	Current Density	V <sub>act</sub>	Activation Voltage
J <sub>max</sub>	Current Density (Max)	V <sub>d</sub>	Potential Drop in R <sub>a</sub>
N <sub>s</sub>	Series Number	V <sub>conc</sub>	Concentration Voltage Drop
N <sub>p</sub>	Parallel Number	V <sub>ohmic</sub>	Ohmic Voltage Drop
P <sub>H2</sub>	Partial Pressure, H <sub>2</sub>	V <sub>FC</sub>	FC Voltage
P <sub>O2</sub>	Partial Pressure, O <sub>2</sub>	V <sub>stack</sub>	Stack Voltage
Y <sub>HO</sub>	Flow Rate H <sub>2</sub> , O <sub>2</sub>	K <sub>r</sub>	Modeling Constant
T <sub>o2</sub>	Time constant, O <sub>2</sub>	T <sub>OH2</sub>	Time constant, H <sub>2</sub>

Saturation loss or material transfer occurs when hydrogen and oxygen have problems reaching the electrodes. This problem is usually more severe in the cathode. Because the reaction is exothermic, the water produced from the reaction usually boils and the vapors produced prevent sufficient oxygen from reaching the cathode [28, 29]. In practice, this problem is reduced by considering the cooling mechanism in the cathode. In order to model the effect of saturation losses on the output voltage of the cell, (4) is used [6]. In this equation:

$$V_{conc} = \frac{-RT}{2F} \cdot \ln \left( 1 - \frac{I}{I_{limit}} \right) \quad (4)$$

Where  $I$  is FC Current (A),  $I_{limit}$  is Lowest Allowed Current (A)

The ohmic voltage drop is caused by such things as the internal resistance of the electrolyte against the passage of energy carriers, as well as the resistance of the electrodes and other internal connections of the cell [30, 31]. Value of ohmic resistance ( $R_{ohm}$ ) is a function of cell temperature and current and is calculated by (5) [2].

$$R_{ohm} = R_0 + KRI - KRTT \quad (5)$$

Where  $R_0$  is Fixed value in ohms,  $KRI$ ,  $KRT$  is the experimental constants are in ohms per ampere and ohms per kelvin, respectively.

Considering the chemical nature of the relations necessary for the thermal modeling of the fuel cell, the details of its modeling have been avoided.

In this article, from the dynamic model presented in [32] to simulate the PEM (Proton Exchange Membrane) FC performance used. The electrical equivalent circuit of PEM fuel cell is shown in Fig. 3.

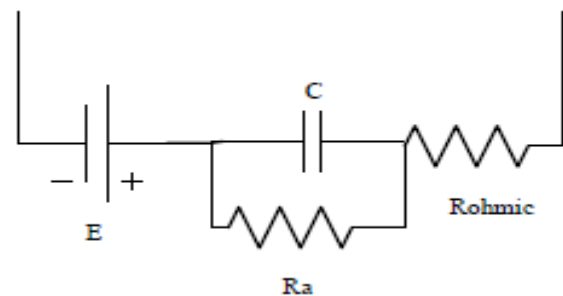


Fig. 3. Electrical equivalent circuit of a FC with a double charge capacitor

The resistance  $R_a$  in Fig. 3 represents the sum of concentration and activation resistances and is equal to: [2]

$$R_a = \frac{V_{act} + V_{conc}}{I_{FC}} \quad (6)$$

Finally, the voltage of a FC stack consisting of  $N_s$  series cells is equal to: [33]

$$V_{stock} = N_s.V_{FC} \quad (7)$$

The relationships and mathematical equations written for the FC system in the relationships mentioned above, which show the performance and model of the polymer fuel cell, are given and simulated in the computer software. The

dynamic model of solid oxide fuel cell is done based on electrochemical and thermodynamic specifications of solid oxide fuel cells [34, 35]. The output voltage of the cell depends on the combination of the fuel, oxide and fuel current, pressure and temperature of cathode and anode, the thermal feature of the cell, electrical features of the cell, cell temperature and charge flow. Fig. 4 shows the Overview of a SOFC; system [36].

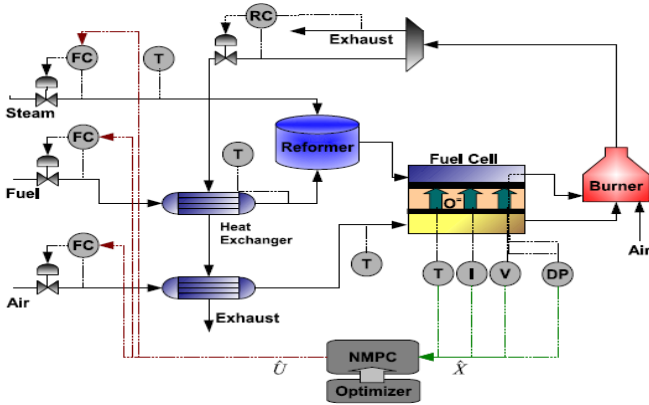


Fig. 4. Overview of a SOFC; system

As shown in Fig. 4, A fuel cell system consists of many components. Components are built around the fuel cell to maximize system efficiency, which depending on the purpose may include additional heat exchangers, turbines, boilers, DC-AC converters, etc. Optimal operation of the system thus requires efficient operation of these integral components, which put constraints on the overall operation of the fuel cell system [37]. The block diagram representation of the SOFC dynamic model is shown in the Fig. 5 [38, 39].

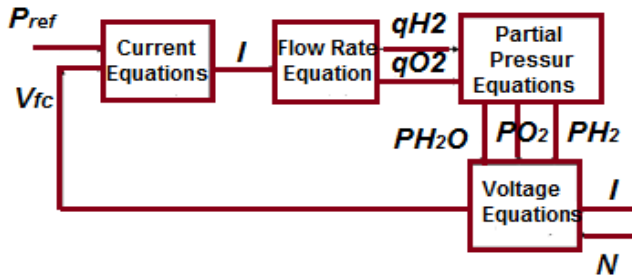


Fig. 5. Block diagram for dynamic model of SOFC

### III. THE PROPOSED METHOD FOR DYNAMIC SIMULATION OF SOFC

This section is aimed to introduced a usable algorithm for dynamic simulation of the mentioned fuel cells. The given algorithm is of 4 stages which are explained deliberately in the following [40, 41].

#### A. Stage 1: data creation for test and training

Data creation which covers different working parts of fuel cells is required for smart system training. Additionally, dynamic modeling requires dynamic data for training. Dynamic data are created using PRBS signals. The given data can be used for smart system training. The current paper uses support vector machines and artificial neural networks for dynamic modeling of black box. PRBS signal is detected

using the known approaches used for data creation required by dynamic modelling process. Ref. [42, 43] show that the given signal is of a wide frequency range and its autocorrelation function is approximating white noise. For dynamic modeling, the mentioned signal is enforced to the selected inputs. This way, created data are used for smart system training.

#### B. Stage 2: selection of the appropriate inputs based on decision tree

According to the specification of decision tree, final parameters for training are selected. In this way, input data required for training are lessened. However, the parameters of the highest effect on output are selected for training [44].

#### C. Stage 3: smart system training with the selection of the best parameters

This stage is aimed at determining the hidden layers or neurons (for artificial neural network) or required parameters (support vector machines) in order to minimize error of voltage prediction [45]. Three indices including ME and MSE and SCC are used for evaluation. These indices are elaborated in stage 4.

#### D. Stage 4: evaluation of the proposed model based on the test data

Prediction error of smart models are investigated using ME, MSE and SCC. The mentioned indices are described as:

$$ME = \text{Max}|V_{act,i} - V_{pre,i}| \quad i = 1, 2, \dots, T \quad (8)$$

Where  $V_{act,i}$  represents actual output voltage for  $i$ th point.  $V_{act,i}$  is the model output.  $T$  shows the points of test data [46].

$$MSE = \frac{1}{T} \sum_{i=1}^T (V_{act,i} - V_{pre,i})^2 \quad (9)$$

$$SCC = 1 - \frac{SS_{err}}{S_{tot}} \quad (10)$$

$$SS_{tot} = \sum_{i=1}^T (V_{act,i} - V_{act})^2 \quad (11)$$

$$SS_{err} = \sum_{i=1}^T (V_{act,i} - V_{pre,i})^2 \quad (12)$$

$$\bar{V}_{act} = \frac{1}{T} \sum_{i=1}^T V_{act,i} \quad (13)$$

A model of better ability in voltage prediction makes Maximum Error (ME) and Mean Square Error (MSE) approach zero and Squared Correlation Coefficient (SCC) approach 1. Mathematical model of data mining is used for smart modeling. Results of the smart models trained by the given algorithm and results of the mathematical model mentioned in [47] are compared in the following sections.

To see the characteristics of a FC that has a maximum power point, instead of a constant current of 5A, we choose a ramp with slope = 0.01 and set the simulation time to 15800 sec. At this time, the amount of current reached from zero to 158A and the waveform of output voltage (Fig. 7), output power (Fig. 8), ohmic voltage drop (Fig. 9), activity and concentration as well as partial pressure effective on H<sub>2</sub>O (Fig. 10 and Fig. 11) are shown.

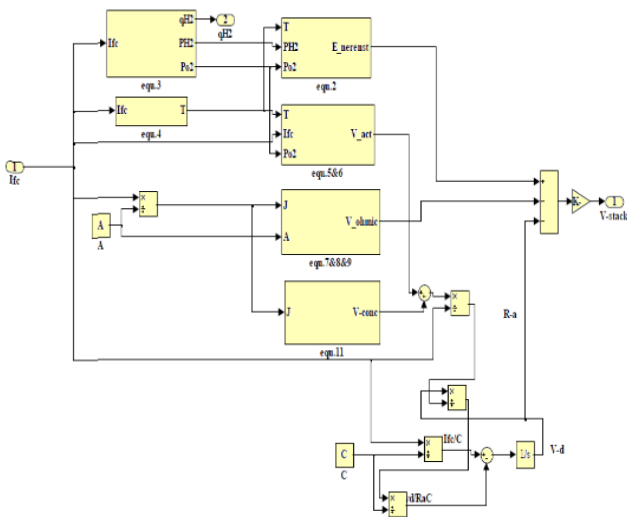


Fig. 6. General block of polymer FC simulation

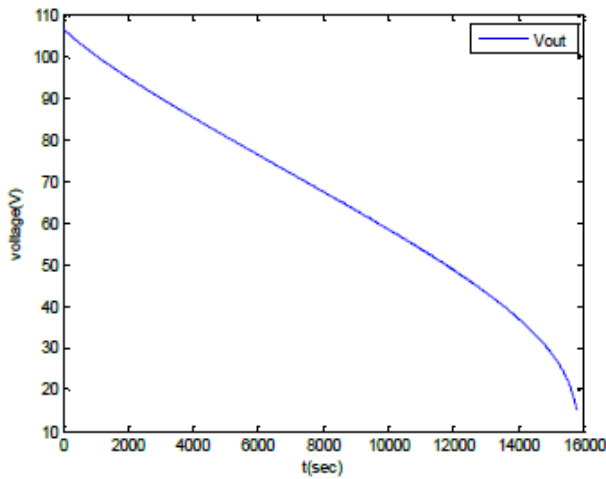


Fig. 7. FC output voltage

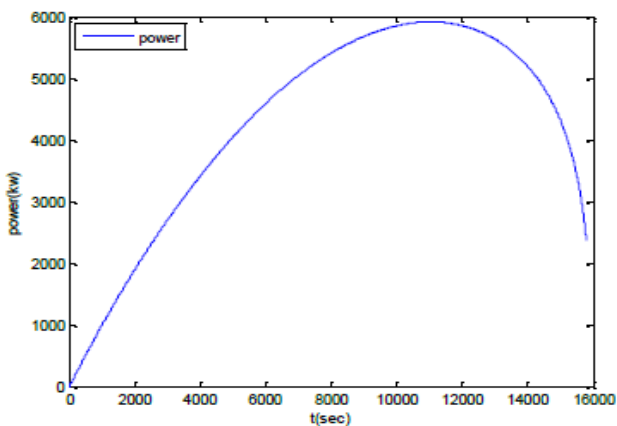


Fig. 8. FC output power

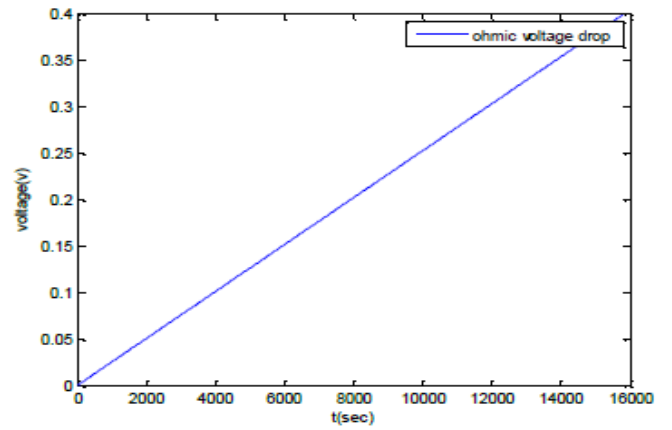


Fig. 9. Ohmic voltage drop

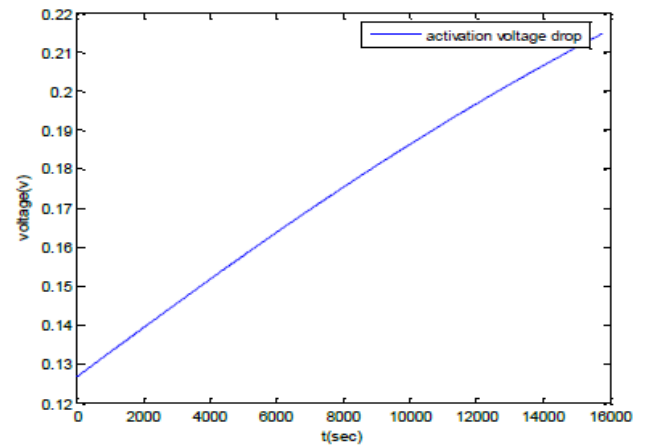


Fig. 10. Activity voltage drop

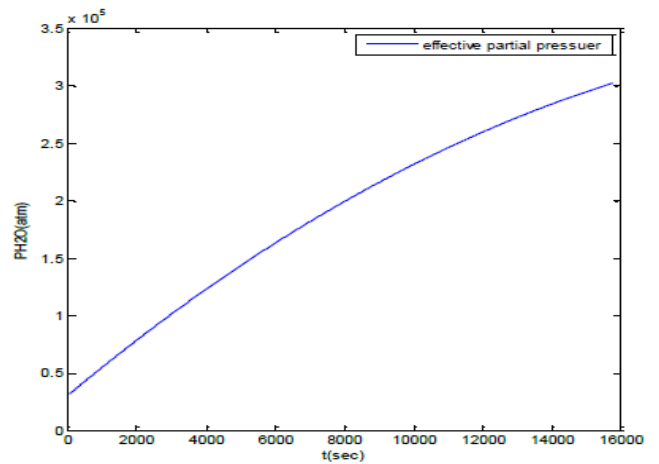


Fig. 11. Effective partial pressure  $H_2O$

#### IV. SYSTEM STRUCTURE

##### A. The Necessity of Power Control for Micro grid

Since in micro grids, the number of DG sources and their power are limited (due to environmental and economic constraints), therefore the inertia of the system is low. In island mode, this factor causes a small abnormality in power to cause a large fluctuation in frequency. For this reason, there is a need for power control in micro grid operation. In

the case of connecting to the grid, considering the economic issues, it is necessary to control the active and reactive power transmitted to the main grid at different hours. Power control can be done in two different ways: Generated power control by DG sources- Load control. Considering that in this article the control of the generated power is considered, A power controller has been developed to control the active and reactive power of the network including the fuel cell, and the simulation results show the effectiveness of this system for power control in the mode of connection to the network.

### B. Power Control in the Grid Considering the Limitations of DG Resources

In this section, we present the impact of the distributed generation limitation on the control of distributed generation sources and as a result, the network power control. Each of the units in the micro grid network according to Fig. 12 consists of a primary driver such as a gas turbine, fuel cell, etc., a battery and an inverter.

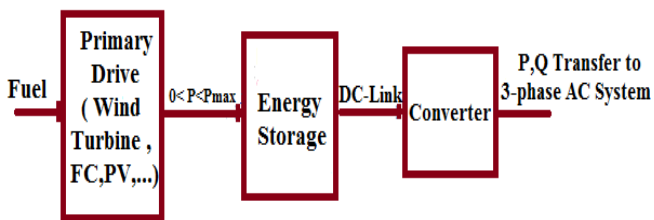


Fig. 12. Main Components of a DG Unit

In this case, the power generation by each unit is highly dependent on the condition of the battery. This means that if the battery is less than its maximum charge, then when the power generating source injects into the network, some of its power must be consumed and the battery charged. That is, if the battery is fully charged, it will be disconnected from the DG source terminal. Otherwise, it uses some of the generated power of the DG source for its charging. The rate of power passing through the inverter is also considered to be slightly higher than the maximum output of the power source. And if the power passing through the inverter is more than the maximum power that can be passed, Protection devices cut off the generator from the grid. Another important thing about inverters is that they are able to pass power in both directions, that is, both active and reactive power flows from the unit to the grid, and from the grid, the power can be multiplied.

### C. Control of FC Power in Grid Connection Mode

Control of FC can be done under the following conditions: Following the maximum power point -Operating at the maximum efficiency - using at the optimal utilization point (approximately 80 to 90 percent). Any control method used for a FC must consider the following limitations: If the fuel efficiency falls below a certain limit, the voltage will increase rapidly - If the fuel efficiency exceeds a certain limit, the FC may be damaged due to saturation. According to the V-I characteristic, the FC has a lower limit for the voltage, which if the voltage drops below that limit, it will drop stepwise and as a result, the current will increase stepwise.

## V. VOLTAGE COLLAPSE

Voltage collapse is a complex subject that has been challenging the power system engineers in the past two

decades [48]. Voltage stability is turning into one of the most vital issues inside the strength structures due to the extensive use of the transmission networks Voltage stability refers to the ability of the power system to maintain an acceptable bus voltage under normal conditions, and after disturbances [48].

The accurate illustration of the voltage instability phenomena requires a detailed model of power system additives (generators, transformers, loads and others) [49]. The risk of voltage instability of a power machine can be measured via the gap of the consistent-nation power go with the flow equations from the initial point of operation (base case) to its saddle-node bifurcation point, referred to as the voltage collapse point. This distance is generally known as the balance margin [14–15]. From a physical factor point of view, the stability margin of an electrical device can be matched by some of the functions of the power grid, such as generator voltage, device weight, or the period of demand imbalance in the power system. One crucial reality when reading voltage disintegrate phenomena is that the voltage balance of an electric electricity machine undergoes deterioration while reactive electricity era limits are reached [16]. Nonetheless, in most instances, voltage stability stays whilst a unit reaches its reactive electricity technology restriction (maximum or minimum) [17].

Nevertheless, in noticeably loaded instances on occasion, the steadiness margin well-known shows a discontinuous increase while a generator reaches its reactive strength technology most or minimum limit, but the equilibrium factor belongs to the risky branches of the nostril curves. Consequently, the strength gadget becomes immediately risky because of any inevitable small perturbation, and a dynamic voltage fall apart leading to blackout may also observe [50].

A V-Q curve directly assesses the shortage of reactive supply. We can use V-Q curves effectively to add reactive load at a bus in a manner similar to the outage of reactive supply from a generator or outage of the line charging shunts of medium or long transmission lines and to preventing voltage collapse in power system. In [19] V-Q curve has been used in the voltage stability assessment method. A V-P curve is quite valuable for assessing transmission or loading constraints. Furthermore, V-P curves cannot as effectively identify regions where reactive shortages occur for generator or line outages [20].

## VI. V-I CURVES OF FCs

Voltage-current density curves of five type of fuel cell (PEFC, AFC, PAFC, MCFC, and SOFC) are shown in [21]. Many parameters such as temperature,  $O_2$  pressure, and effect on fuel cell performance in [22] had described. Fig. 13 shows a typical variation of the output voltage of a fuel cell stack in response to changes in load current [23]

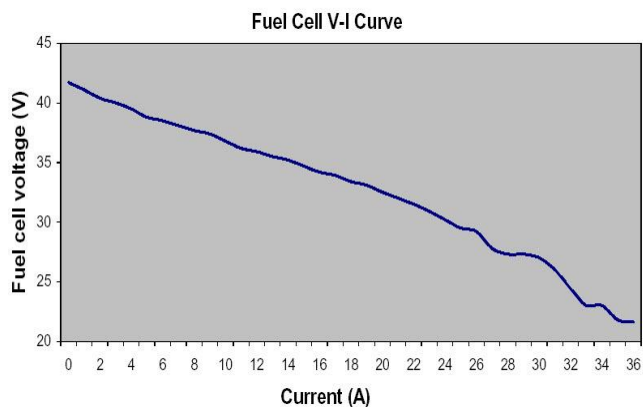


Fig. 13. Typical fuel cell voltage / current characteristics

VII. APPLICATION OF FUEL CELL DISTRIBUTED GENERATION (FCDG)

The use of distributed generation sources has many advantages, including meeting the peak load needs, reducing network losses, providing reactive power locally, and regulating the network voltage [24]. Of all the distributed generation sources, fuel cells are of particular importance due to their high efficiency, high energy density, ability to simultaneously generate heat and electrical power, and low emission of pollutants. In this paper, the use of a fuel cell system connected to the grid as a distributed source with high reliability is proposed, and the dynamic model of the fuel cell is simulated. boost DC / DC converter, is commonly used to increase the output voltage level of the system and stabilize the DC link voltage. This converter can connect multiple sources of distributed generation and provides different in parallel, which is without the need for synchronization. Figure 6 shows the general power structure of the converter proposed for controlling the FC system. The network side converter (inverter connected to the network) is responsible for controlling the active and reactive power produced by the system [25]. This goal has been achieved by applying the vector controls method to the converter on the network side, the most essential feature is the fast dynamics in responding to changes [26].

A. Power Condition Unit (PCU)

The output voltage of the FC in series stacks is an uncontrolled DC voltage that fluctuates with load changes. This voltage must be converted to a controlled DC voltage. The PCU controls the electrical frequency. It keeps the harmonics at an acceptable level. The overall configuration of the system includes a FC, after which a boost converter is placed, it also includes a battery bank, which is placed after the battery, bidirectional converter and then an inverter. The obtained controlled voltage is sent to the DC/AC inverter after being filtered [27]. The boost converter is placed as an intermediary between the fuel cell system and the inverter system. Fuel cell systems connected to the network include a storage battery. This topology is shown in Fig. 14.

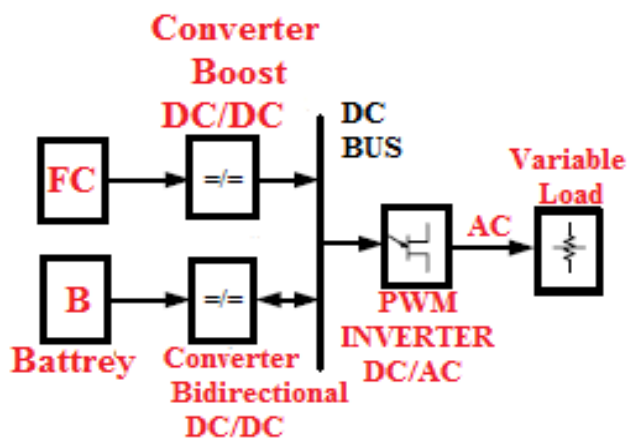


Fig. 14. Topology of Network connection

B. DC/DC Boost Converter

The power converter must protect the converter system against output fluctuations, reverse currents and sudden load changes and guarantee its full life. The output voltage is always greater than the input voltage. Battery-powered devices use a DC/DC step-up converter to produce a higher voltage than the battery voltage. The main advantage of the boost converter, the efficiency is high and the number of components is small, and it can convert the unregulated voltage into the desired regulated voltage by changing the duty cycle at a high switching frequency and reduce the size and cost of energy storage components [26, 27].

C. Bi-directional Converters

Battery and supercapacitor lines are used as energy storage to quickly respond to rapid load changes that could not be followed by the fuel cell and cause a delay in the cold start of the fuel cell. The circuit diagram of the proposed bidirectional controllable DC converter, in this topology, is shown in Fig. 15. The two main switches S1, S2 are from the same converter leg. And they are controlled by the gate signals, based on the operation mode of the circuit. When the direction of power distribution is towards low-voltage (battery), the converter works like a buck converter. When the power distribution is in the reverse direction, the converter acts as a boost converter. In each of the working modes, a switch and reverse parallel diode work at the other two ends of the switch [28].

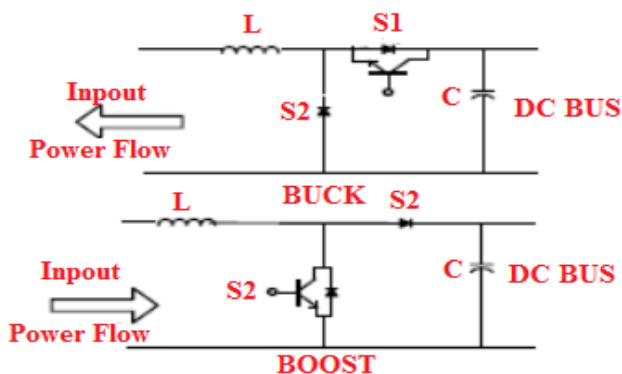


Fig. 15. Topology Models of Bidirectional DC converter

VIII. SIMULATIONS RESULTS

Several years ago, studies about using small gas turbines and high-temperature FCs; with heat exchangers to gather to produce electrical power and heat stimulatingly had increased. Hence in this section, we show the effect of FCs; over V-Q and V-P curves of a single machine (small gas turbine) system with simulating it in Dig Silent area. Fig. 16 shows a single machine (DG;) system, and Fig. 17 & Fig. 18 show the V-Q curves of a single machine system. Fig. 19, Fig. 20, Fig. 21 show the V-P curves of the simulated system. With change PF; as PF=0.7, 0.8, 0.9, 1, and without FC. We investigate the effect of FC for some PFs, and the results are shown in Figs. 19-23. Different PF obtained with control P & Q of FC. Some characteristics of devices are presented in Table 2. In this section, changes in the reference value for active and reactive power were applied to the system, and the results for the controller along with the reference power are shown in Fig. 24 and Fig. 25.

Parameter change can happen for any system and have a negative impact on the controller and the purpose for which the controller is designed. Therefore, the robustness of the controller to changing system parameters can be considered one of the advantages of a good controller. For our studied system, the change of the considered parameter is the change in the value of the inductor connecting the FC to the grid. This parameter changes in 0.5 seconds to apply to the system and the results can be seen according to Fig. 26 and Fig. 27.

TABLE II. SOME CHARACTERISTICS OF DEVICES

devices	Parameters
G	S=4.855MVA, V=10.5kv, PF=0.8, xd=0.5, xq=0.75
FC	S=5MVA
LOAD	P=2MW, Q=0.78MVar
LINE	L=100km, R=0.05811Ω/km, X=0.17632 Ω/km

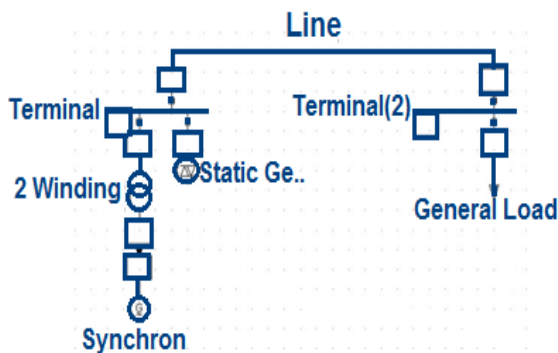


Fig. 16. Design of Single machine with Dig Silent.

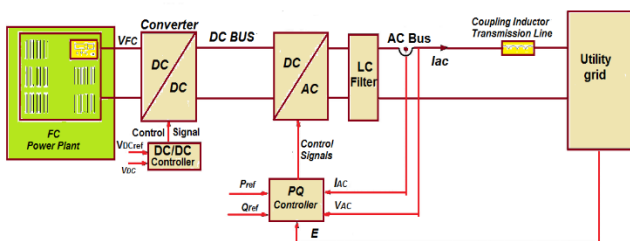


Fig. 17. Block diagram of a Fuel Cell Distributed Generation system

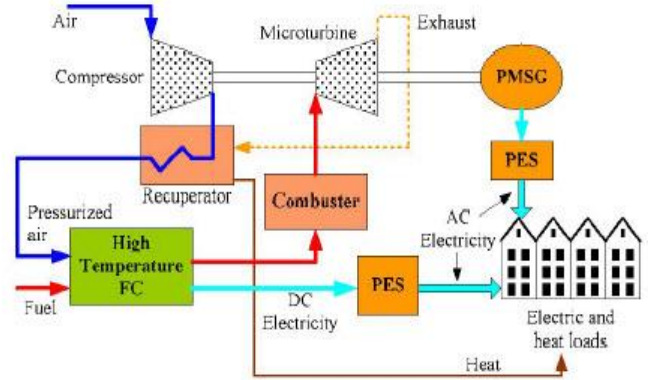


Fig. 18. schematic block diagram of an FCMT combined heat and power generation.

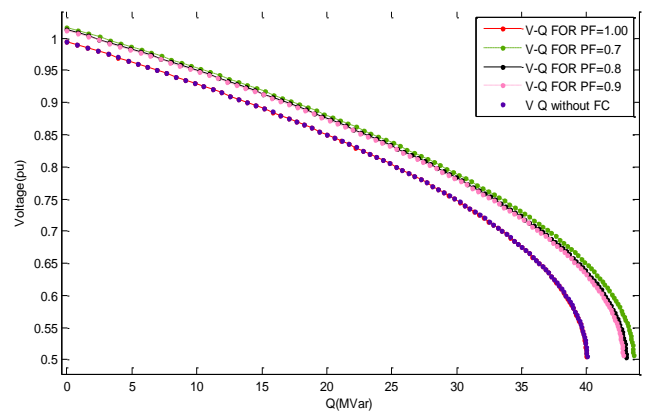


Fig. 19. V-Q curves for different PF of FC

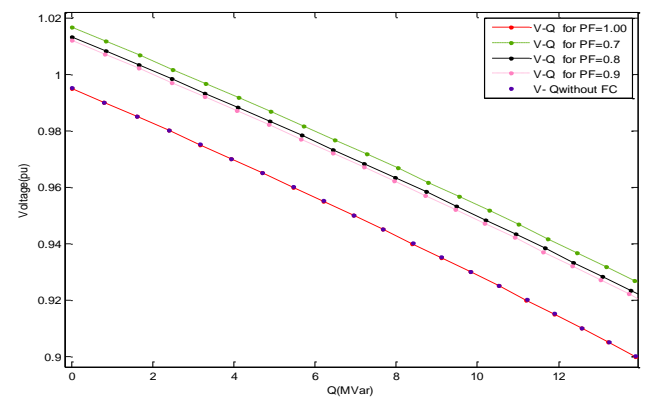


Fig. 20. V-Q curves for different PF of FC (Zoom)

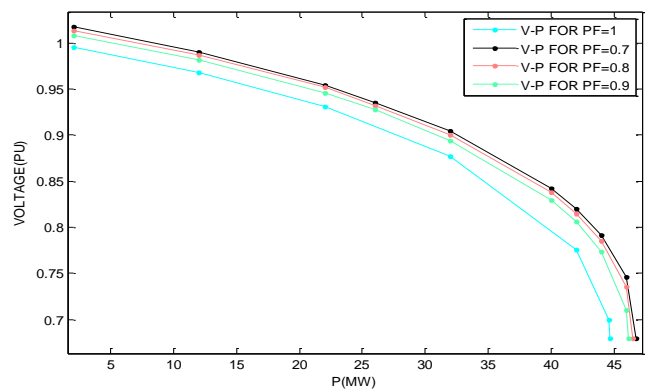


Fig. 21. V-P curves for different PF of FC



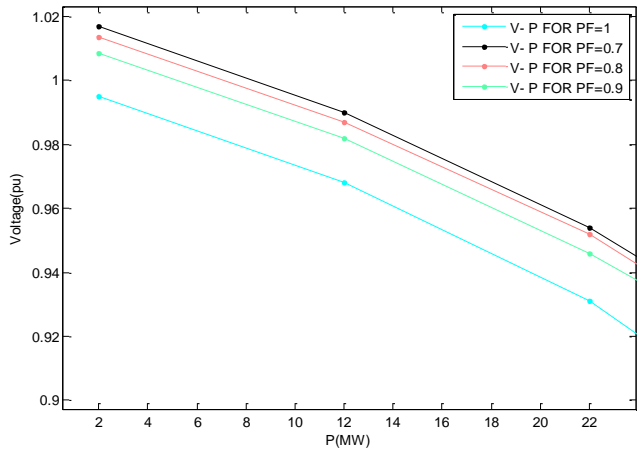


Fig. 22. V-P curves for different PF of FC (Zoom)

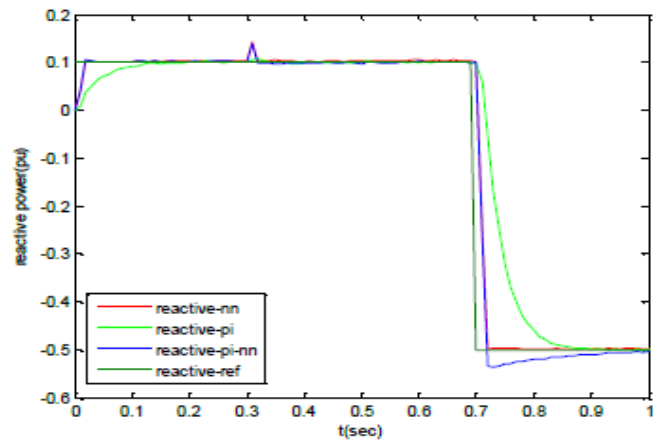


Fig. 25. Comparison of Reference Reactive Power with the Controller Output

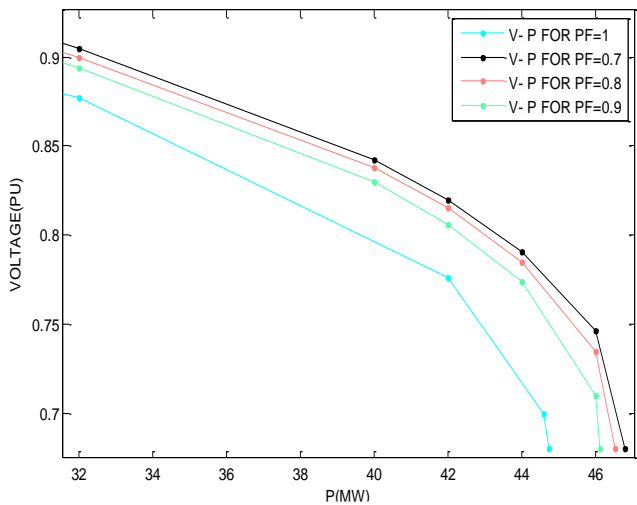


Fig. 23. V-P curves for different PF of FC (Zoom)

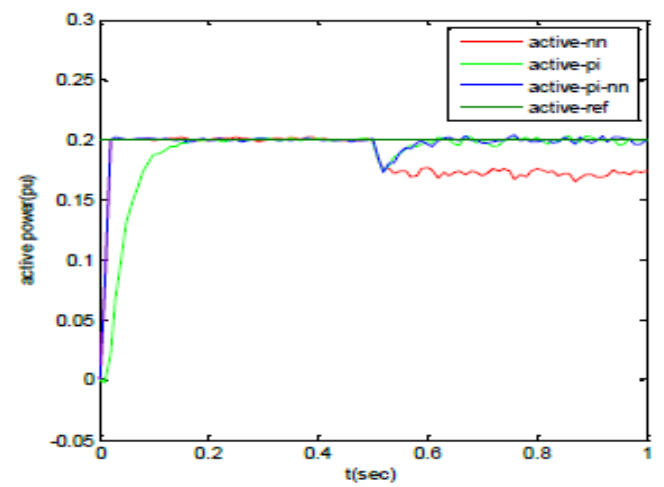


Fig. 26. Comparison of robustness of controllers in tracing active power after system parameter change in 0.5 seconds

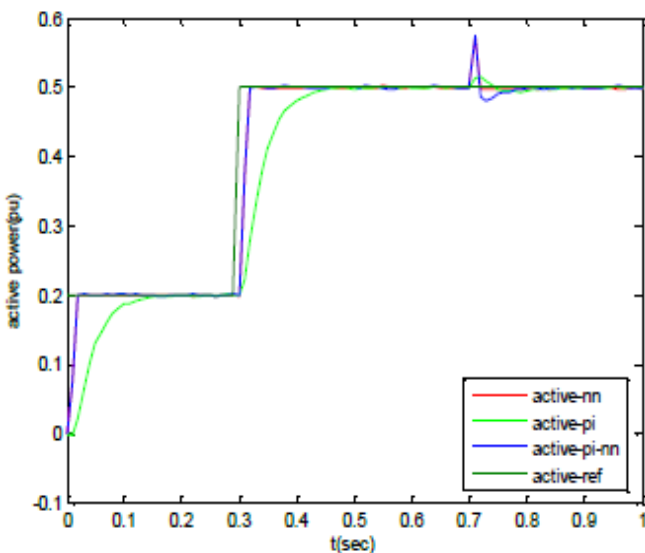


Fig. 24. Comparison of reference active power with controller output

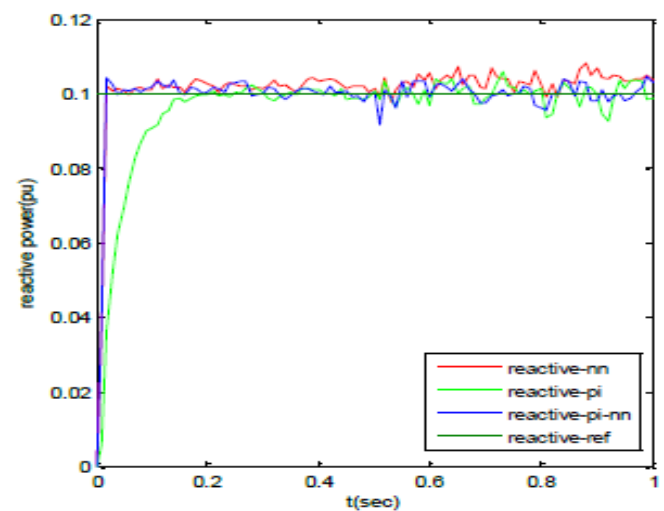


Fig. 27. Comparison of the robustness of the controllers in following the reactive power after system parameter change in 0.5 sec

### IX. CONCLUSION

Voltage collapse phenomena are highly affected by reactive power generation limits. Increasing and saturating the reactive power of a unit may lead to a deterioration of

voltage stability. However, in some cases, when the power network is operating close to the voltage collapse point, the reactive power generation saturation of a unit can change the system voltages immediately from stable to unstable; thus, a dynamic voltage collapse leading to a blackout may follow [10], thus with using a controller for control the active and reactive power of FCs in power network, voltage stability margin will be improved. Furthermore, fuel cells (FCs) have several advantages and can be used in any application to generate heat and electrical power simultaneously. As Fig. 19, Fig. 20, Fig. 21, Fig. 22 showed, with control the PF of the FC, we can change the V-Q and V\_P curves, respectively. Therefore in this paper, we acclaim that by controlling the active and reactive power of a coupled FC to the small gas turbine, we can improve the V-P and V-Q curves of the overall system. Active and reactive power of FC controlled with the controller as presented in Fig. 6.

#### REFERENCES

- [1] V. Balamourougan, T. S. Sidhu and M. S. Sachdev, "Technique for online prediction of voltage collapse," *IEE Proc.-Gener. Transm. Distrib.*, vol. 151, no. 4, 2004.
- [2] M. Movahedpour, M. J. Kiani, M. Zadehbagheri and S. Mohammadi, "Microgrids Operation by Considering Demand Response and Supply Programs in the Presence of IGDT-Based Reverse Risk," in *IEEE Access*, vol. 10, pp. 48681-48700, 2022.
- [3] IEEE Working Group on Voltage Stability, "Suggested Techniques for Voltage Stability Analysis," IEEE Power Engineering Society Report, 93TH0620-5PWR, 1993.
- [4] C. Wang, M. H. Nehrir and H. Gao, "Control of PEM Fuel Cell Distributed Generation System," *IEEE transactions on Energy Conversion*, vol. 21, no. 2, pp. 586-595, 2006.
- [5] C. Wang, M.H. Nehrir, "A Dynamic SOFC Model for distributed Power Generation Applications," 2005 Fuel Cell Seminar, pp. 14-18, 2005.
- [6] C. Wang, M. H. Nehrir and S. R. Shaw, "Dynamic Models and Model Validation for PEM Fuel Cells Using Electrical Circuits," *IEEE transactions on Energy Conversion*, vol. 20, no. 2, pp. 442-451, 2005.
- [7] A. Javadian, M. Zadehbagheri, M. J. Kiani, S. Nejatian, "Comprehensive modeling of SVC-TCSC-HVDC power flow in terms of simultaneous application in power systems," *Journal of Power Electronics*, vol. 21, pp. 1493-1507, 2021.
- [8] Q. Xun, Y. Liu, J. Zhao and E. A. Grunditz, "Modelling and Simulation of Fuel Cell/ Supercapacitor Passive Hybrid Vehicle System," 2019 IEEE Energy Conversion Congress and Exposition (ECCE), pp. 2690-2696, 2019.
- [9] H. Janben, J. Supra, and W. Lehnert, "Stack concepts for high temperature polymer electrolyte membrane fuel cells," *High Temp. Polym. Electrolyte Membr. Fuel cells.*, 2016, p. 441e57.
- [10] F. M. Echavaren, E. Lobato, and L. Rouco, "Steady-state analysis of the effect of reactive generation limits in voltage stability," *Electric Power Systems Research*, vol. 79, pp. 1292-1299, 2009.
- [11] C. A. Canizares, "on bifurcations, voltage collapse and load modeling," *IEEE Transactions on Power Systems*, vol. 10, no. 1, pp. 512-522, 1995.
- [12] V. Acevedo, M. Walter, "Long-term voltage stability monitoring of power system areas using a kernel extreme learning machine approach," *Alexandria Engineering Journal*, vol. 61, no. 2, pp. 1353-1367, 2022.
- [13] I. Dobson, H. Glavitsch, C.C. Liu, Y. Tamura, V. Vu, "Voltage collapse in power systems," *IEEE Circuits and Devices Magazine*, vol. 8, no. 3, pp. 40-45, 1992.
- [14] Z. Feng, V. Ajjarapu, B. Long, "Identification of voltage collapse through direct equilibrium tracing," *IEEE Transactions on Power Systems*, vol. 15, no.1, pp. 342-349, 2000.
- [15] M. Zadehbagheri, et al, "Design of a new backstepping controller for control of microgrid sources inverter," *Int. J. Electr. Comput. Eng.*, Vol. 12, No. 4, August 2022, pp. 4469-4482, doi: 10.11591/ijece.v12i4.pp4469-4482.
- [16] H. Eskandari, M. Kiani, M. Zadehbagheri, "Optimal scheduling of storage device, renewable resources and hydrogen storage in combined heat and power microgrids in the presence plug-in hybrid electric vehicles and their charging demand," *Journal of Energy Storage*, vol. 50, 2022.
- [17] I. Dobson, L. Lu, "Voltage collapse precipitated by the immediate change in stability when generator reactive power limits are encountered," *IEEE Transactions on Circuits and Systems I: Fundamental Theory and Applications*, vol. 39, no. 9, pp. 762-766, 1992.
- [18] G. Pongratz, "Solid oxide fuel cell operation with biomass gasification product gases: Performance and carbon deposition risk evaluation via a CFD modelling approach," *Energy*, vol. 244, 2022.
- [19] E. Faraji, A. Abbasi, S. Nejatian, M. Zadehbagheri, and H. Parvin, "Probabilistic planning of the active and reactive power sources constrained to securable-reliable operation in reconfigurable smart distribution networks," *Electric Power Systems Research*, vol. 199, 2021.
- [20] K. Deng, "Deep reinforcement learning based energy management strategy of fuel cell hybrid railway vehicles considering fuel cell aging," *Energy Conversion and Management*, vol. 251, 2022.
- [21] N. Akhtar, S. P. Decent, D. Loghin, and K. Kendall, "A three-dimensional numerical model of a single-chamber solid oxide fuel cell," *Int. J. Hydrogen Energy*, vol. 34, pp. 8645-8663, 2009.
- [22] R. T. Jagaduri and G. Radman, "Modeling and control of distributed generation systems including PEM fuel cell and gas turbine," *Electr. Power Syst. Res.*, vol. 77, pp. 83-92, 2007.
- [23] R. bovea, P. Lunghi, and N. M. Sammes, "SOFC mathematic model for systems simulations-Part 2: definition of an analytical model," *Int. J. Hydrogen Energy*, vol. 30, no. 2, pp. 189 - 200, 2005.
- [24] S. K. Nayak, A. T. Hoang, S. Nižetić, X. P. Nguyen, and T. H. Le, "Effects of advanced injection timing and inducted gaseous fuel on performance, combustion and emission characteristics of a diesel engine operated in dual-fuel mode," *Fuel*, vol. 310, pp. 122-232, 2022.
- [25] P. Barnoon, D. Toghraie, B. Mehmandoust, M. A. Fazilati, and S. A. Eftekhari, "Natural-forced cooling and Monte-Carlo multi-objective optimization of mechanical and thermal characteristics of a bipolar plate for use in a proton exchange membrane fuel cell," *Energy Reports*, vol. 8, pp. 2747-2761, 2022.
- [26] J. Yang, X. Li, J. H. Jiang, L. Jian, L. Zhao, J. G. Jiang, X. G. Wu, and L. H. Xu, "Parameter optimization for tubular solid oxide fuel cell stack based on the dynamic model and an improved genetic algorithm," *Int. J. Hydrogen Energy*, vol. 36, pp. 6160-6175, 2011.
- [27] Y. Wang, J. Xu, H. Zang, and Z. Wang, "Synthesis and properties of sulfonated poly (arylene ether ketone sulfone) containing amino groups/functional titania inorganic particles hybrid membranes for fuel cells," *International journal of hydrogen energy*, vol. 44, no. 12, March 2019, pp. 6136-6147, doi.org/10.1016/j.ijhydene.2019.01.035.
- [28] A. Kuzmin, "La Sc O3-based electrolyte for protonic ceramic fuel cells: Influence of sintering additives on the transport properties and electrochemical performance," *Journal of Power Sources*, vol. 466, pp. 228-255, 2020.
- [29] M. Chen, C. Zhao, F. Sun, J. Fan, H. Li, and H. Wang, "Research progress of catalyst layer and interlayer interface structures in membrane electrode assembly (MEA) for proton exchange membrane fuel cell (PEMFC) system," *ETransportation*, vol. 5, 2020.
- [30] S. Wang, J. Shen, Z. Zhu, Z. Wang, Y. Cao, X. Guan, Y. Wang, Z. Wei, and M. Chen, "Further optimization of barium cerate properties via co-doping strategy for potential application as proton-conducting solid oxide fuel cell electrolyte," *Journal of Power Sources*, vol. 387, pp. 24-32, 2018.
- [31] W. Chen et al, "On the modelling of fuel cell-fed power system in electrified vessels," In 2020 IEEE, 21st Workshop on Control and Modeling for Power Electronics (COMPEL), IEEE, pp. 1-8, 2020.
- [32] V. I. Vishnyakov, "Pulsed high-voltage electrical discharges in water: The resource for hydrogen production and water purification," *International Journal of Hydrogen Energy*, vol. 47, no. 25, pp. 12500-12505, 2022.
- [33] I. M. Alvarez, E. Zarrabeitia-Bilbao, R. M. Rio-Belver, and G. Garechana-Anacabe, "Fuel-cell electric vehicles: Plotting a scientific and technological knowledge map," *Sustainability*, vol. 12, no. 6, 2020.
- [34] C. P. Sherwood, D. C. Elkington, M. R. Dickinson, W. J. Belcher, P. C. Dastoor, K. Feron, A. M. Brichta, R. Lim, M. J. Griffith,

- "Organic semiconductors for optically triggered neural interfacing: The impact of device architecture in determining response magnitude and polarity," *IEEE Journal of Selected Topics in Quantum Electronics*, vol. 27, no. 4, 2021.
- [35] M. J. Leeuwner, A. Patra, D. P. Wilkinson, E. L. Gyenge, "Graphene and reduced graphene oxide based microporous layers for high-performance proton-exchange membrane fuel cells under varied humidity operation," *Journal of Power Sources*, vol. 423, pp. 192-202, 2019.
- [36] L. Kistner, A. Bensmann, and R. Hanke-Rauschenbach, "Optimal design of power gradient limited solid oxide fuel cell systems with hybrid storage support for ship applications," *Energy Conversion and Management*, vol. 243, p. 114396, 2021.
- [37] Y. Chellehbari, "A numerical simulation to effectively assess impacts of flow channels characteristics on solid oxide fuel cell performance." *Energy Conversion and Management*, vol. 244, 2021.
- [38] N. Etherden and M. H. J. Bollen, "Increasing the hosting capacity of distribution networks by curtailment of renewable energy resources," *IEEE Trondheim PowerTech*, pp. 1-7, 2011.
- [39] A. Shirsath, S. Raael, C. Bonnet, L. Schiffer, W. Bessler, F. Lapique, "Electrochemical pressure impedance spectroscopy for investigation of mass transfer in polymer electrolyte membrane fuel cells," *Curr. Opin. Electrochem*, vol. 20, pp. 82-87, 2020.
- [40] S. Keller, T. Oezel, A. C. Scherzer, D. Gerteisen, U. Gross, C. Hebling, Y. Manoli, "Characteristic Time Constants Derived from Low Frequency Arc of Impedance of Fuel Cell Stack," *J. Electrochem. Energy Convers. Storage*, vol. 15, pp.1-10, 2018.
- [41] J. Correa, F. A. Farret, J., Gomes, M. G. Simoes, "Simulation of Fuel-Cell Stacks using a Computer-Controlled Power Rectifier With the Purposes of Actual High-Power Injection Application," *IEEE Transactions on Industry Applications*, vol. 39, no. 4, pp. 1136-1142, 2003.
- [42] A. A. Ebrahimzadeh, I. Khazaei, A. Fasihfar, "Numerical investigation of obstacle's effect on the performance of proton-exchange membrane fuel cell: studying the shape of obstacles," *Heliyon*, vol. 21, no. 5, 2019.
- [43] Y. Kerkoub, A. Benzaoui, F. Haddad, K. YasminaZiari, "Channel to rib width ratio influence with various flow field designs on performance of PEM fuel cell," *Energy Convers. Manag.*, vol. 174, pp. 260-275, 2018.
- [44] A. Baricci, R. Mereu, M. Messaggi, M. Zago, F. Inzoli, A. Casalegno, "Application of computational fluid dynamics to the analysis of geometrical features in PEM fuel cells flow fields with the aid of impedance spectroscopy," *Appl. Energy*, vol. 205, pp. 670-682, 2017.
- [45] S. Cheng, D. Hu, D. Hao, Q. Yang, J. Wang, L. Feng, and J. Li, "Investigation and analysis of proton exchange membrane fuel cell dynamic response characteristics on hydrogen consumption of fuel cell vehicle," *International Journal of Hydrogen Energy*, vol. 47, no. 35, pp. 15845-15864, 2022.
- [46] Z. Li, Q. He, C. Wang, Q. Xu, M. Guo, I. T. Bello, and M. Ni, "Ethylene and power cogeneration from proton ceramic fuel cells (PCFC): A thermo-electrochemical modelling study," *Journal of Power Sources*, vol. 536, 2022.
- [47] L. Dong, R. Zhou, "Effect of rotational speed on unstable characteristics of lobe hydrogen circulating pump in fuel cell system," *International Journal of Hydrogen Energy*, vol. 47, no. 50, pp. 21435-21449, 2022.
- [48] D. Ouyang, F. Wang, J. Hong, D. Gao, and X. Zhao, "Ferricyanide and vanadyl (V) mediated electron transfer for converting lignin to electricity by liquid flow fuel cell with power density reaching 200 mW/cm<sup>2</sup>," *Applied Energy*, vol. 304, p. 117927, 2021.
- [49] C. Cosse, M. Schumann, D. Becker, and D. Schulz, "Simulation of electric field control effects on the ion transport in proton exchange membranes for application in fuel cells and electrolyzers," *International Journal of Hydrogen Energy*, vol. 47, no. 12, pp. 7961-7974, 2022.
- [50] A. M. Abass, D. A. Pavlyuchenko, and Z. S. Hussain, "Survey about impact voltage instability and transient stability for a power system with an integrated solar combined cycle plant in Iraq by using ETAP," *Journal of Robotics and Control (JRC)*, vol. 2, no. 3, pp. 134-139, 2021.